



T.C.  
ORTA DOĞU TEKNİK ÜNİVERSİTESİ  
BİLİMSEL ARAŞTIRMA PROJELERİ KOORDİNASYON BİRİMİ

**Zamana Bağlı Magnetohidrodinamik Akış Probleminin Pertürbe Edilmiş  
Sınır Sahip Dikdörtgen Kanal Kesitinde Sınır Elemanları Metodu ile  
Çözümü**

**Proje No:** GAP-101-2018-2768

Proje Türü: Genel Araştırma Projesi

**SONUÇ RAPORU**

**Proje Yürütücüsü:**  
Canan Bozkaya  
Matematik Bölümü, ODTÜ

**Araştırmacılar**  
Münevver Tezer-Sezgin ve Hande Fendoğlu  
Matematik Bölümü, ODTÜ

Mayıs 2019

ANKARA



## ÖNSÖZ

Bu projede, zamana bağı Magnetohidrodinamik (MHD) problemleri, pertürbe edilmiş sınıra sahip dikdörtgen bir kesitte sınır elemanları metodu ile çeşitli iletkenlik koşulları için farklı temel çözümler kullanılarak çözülmüş ve elde edilen sonuçlar karşılaştırılmalı olarak verilmiştir. Magnetohidrodinamik denklemleri, viskoz, sıkıştırılamayan ve elektrik ileten sıvıların akışı ve manyetik alanlarla arasındaki etkileşimin sonucunda ortaya çıkmaktadır. Proje kapsamında, birbirine bağı magnetohidrodinamik denklemleri öncelikle uygun dönüşümler kullanılarak birbirinden bağımsız konveksiyon-difüzyon denklemlerine dönüştürülüp buna karşılık gelen temel çözümler yardımıyla bölge integrali içeren sınır elemanları yöntemi ve karşılıklı sınır elemanları yöntemi ile çözülmüştür. Ardından, bu konveksiyon-difüzyon denklemleri uygun dönüşümler yardımıyla modifiye edilmiş Helmholtz denklemlerine dönüştürülüp yine karşılık gelen temel çözümler kullanılarak bölge integrali içeren sınır elemanları yöntemi ve karşılıklı sınır elemanları yöntemi ile çözülmüştür. Pertürbe edilmiş sınırın MHD akış ve indüklenmiş manyetik alan üzerindeki etkileri her iki yöntemle elde edilmiş ve sonuçlar karşılaştırılmalı bir şekilde grafiksel olarak farklı Hartmann sayıları için gösterilmiştir. Projenin çıktıları uluslararası bir konferansta sunulmuş ve makale olarak basılmıştır. GAP-101-2018-2768 kodlu projemiz ODTÜ Bilimsel Araştırma Projeleri Koordinasyon Birimi'nce desteklenmiştir.

## İÇİNDEKİLER

Sayfa No

ÖZET	1
ABSTRACT	2
PROJE ANA METNİ	3
YAYINLAR/BİLDİRİLER	5
EKLER	7

## ÖZET

Bu çalışmada viskoz, sıkıştırılamayan, elektrikçe iletken sıvıların zamana bağlı akışı manyetik alan etkisinde ve pertürbe edilmiş sınıra sahip dikdörtgen bir kesitte incelenmiştir. Kesitin üst duvarı küçük bir pertürbasyon parametresi kullanılarak pertürbe edilmiş olup, bu şekilde sıkıştırılmış damarlardaki kan akışını canlandırmak amaçlanmıştır. Problemden, magnetohidrodinamik denklemleri hız ve indüklenmiş manyetik alan cinsinden birbirine bağlı kuple denklemler olup kesit duvarları hareketsizdir ve kesitin yan duvarları yalıtılmış olup alt ve üst duvarları tam iletkenidir. Bölgenin ayrıştırılmasında, bölge integrali içeren sınır elemanları yöntemi ve karşılıklı sınır elemanları yöntemi kullanılmış ve zamanın ayrıştırılmasında geri sonlu fark şeması kullanılmıştır. Birbirine bağlı kuple olan magnetohidrodinamik denklemleri ilk olarak uygun dönüşümler kullanılarak birbirinden bağımsız konveksiyon-difüzyon denklemlerine dönüştürülmüş, ardından da üstel formda bir dönüşüm yardımıyla modifiye edilmiş Helmholtz denklemlerine dönüştürülmüştür. Böylece oluşan denklemler karşılık gelen temel çözümler kullanılarak bölge integrali içeren sınır elemanları yöntemi ve karşılıklı sınır elemanları yöntemi ile çözülmüştür. Her iki yöntemle de elde edilen sonuçlar kararlı halde, farklı Hartmann sayı değerleri ve farklı pertürbasyon parametreleri cinsinden karşılaştırılmıştır.

## ABSTRACT

The unsteady magnetohydrodynamic (MHD) flow of a viscous, incompressible and electrically conducting fluid in a rectangular duct with a perturbed boundary, is investigated. A small boundary perturbation is applied on the upper wall of the duct which is encountered in the visualization of the blood flow in constricted arteries. The MHD equations which are coupled in the velocity and the induced magnetic field are solved with no-slip velocity conditions and by taking the side walls as insulated and the Hartmann walls as perfectly conducting. Both the domain boundary element method (DBEM) and the dual reciprocity boundary element method (DRBEM) are used in spatial discretization with a backward finite difference scheme for the time integration. These MHD equations are decoupled first into two transient convection-diffusion equations, and then into two modified Helmholtz equations by using suitable transformations. Then, the DBEM or DRBEM is used to transform these equations into equivalent integral equations by employing the fundamental solution of either steady-state convection-diffusion or modified Helmholtz equations. The DBEM and DRBEM results are presented and compared by equi-velocity and current lines at steady-state for several values of Hartmann number and the boundary perturbation parameter.

## PROJE ANA METNİ

Bu projede, zamana bağılı Magnetohidrodinamik (MHD) problemleri, pertürbe edilmiş sınıra sahip dikdörtgen bir kesitte sınır elemanları metodu ile çeşitli iletkenlik koşulları için farklı temel çözümler kullanılarak çözülmüş ve elde edilen sonuçlar karşılaştırılmalı olarak verilmiştir. Magnetohidrodinamik denklemleri, viskoz, sıkıştırılmayan ve elektrik iletken sıvıların akışı ve manyetik alanlarla arasındaki etkileşimin sonucunda ortaya çıkmaktadır. Bu tip denklemler, jeotermal enerji elde edilmesi, sıvı metal üretimi ve nükleer füzyon gibi endüstriyel alanlarda uygulamalara sahiptir. Bu denklemler için teorik çözüm sadece problemin basitleştirilmiş formlarında mevcuttur. Ancak bu basitleştirme gerçek uygulama alanlarındaki problemleri tam anlamıyla irdeleyememektedir. Dolayısıyla bu problemin gerçek anlamda incelenebilmesi için efektif nümerik metotlara ihtiyaç duyulmaktadır.

Magnetohidrodinamik problemlerinin çözümleri için literatürde çoğunlukla sonlu elemanlar metodu ve karşılıklı sınır elemanları metotları kullanılmıştır. Mevcut olan çözümlerde bölge genellikle dikdörtgen, kare ya da silindir olup düz sınırlara sahiptir. Yapılan çalışmaların ekserisi zamandan bağımsız olup, zamana bağılı olarak çalışılan karşılıklı sınır elemanları yönteminde ise yalnızca küçük Hartmann değerleri incelenmiştir. Bu proje çalışmasında hem zamana bağılı MHD problemi hem de pertürbe edilmiş sınırı olan bölgede elde edilen hız ve indüklenmiş manyetik alanın davranış değişiklikleri fiziksel olarak incelenmiştir.

Birbirine bağılı kuple olan magnetohidrodinamik denklemleri ilk olarak uygun dönüşümler kullanılarak birbirinden bağımsız konveksiyon-difüzyon denklemlerine dönüştürülmüştür ve bu sınır koşullarının birbirlerine bağımlı hale gelmesine neden olmuştur. Ardından, bu konveksiyon-difüzyon denklemleri uygun dönüşümler yardımıyla modifiye edilmiş Helmholtz denklemlerine indirgenmiştir. Konveksiyon-difüzyon denklemleri, karşılık gelen temel çözümler yardımıyla bölge integrali içeren sınır elemanları yöntemi ile nümerik olarak çözülmüş ve modifiye edilmiş Helmholtz denklemleri de aynı şekilde karşılık gelen temel çözümler kullanılarak bölge integrali içeren sınır elemanları yöntemi ile nümerik olarak

çözülmüştür. Elde edilen çözümler karşılaştırılmış ve anlaşılmıştır ki konveksiyon-difüzyon temel çözümü ile elde edilen sonuçlar daha başarılıdır. Bu sebeple çalışmanın devamında ele alınan uygulama problemlerinde bu temel çözüm kullanılmıştır.

Elde edilen nümerik çözümler literatürde mevcut olan sonuçlar ile karşılaştırılmış ve birbirleriyle büyük bir uyum içinde oldukları gözlenmiştir. Nümerik çözümler elde edilirken  $T=1$  zamanında çözümlerin kararlı hale ulaştığı gözlenmiş ve ilgili grafiklerle desteklenmiştir. Bu sebeple çalışmadaki tüm nümerik hesaplamalar  $T=1$  zamanında yapılmıştır. Farklı pertürbasyon parametreleri için analizler yapılmış ve pertürbasyon katsayısı büyüdükçe hızın azaldığı, indüklenmiş manyetik alanın ise arttığı gözlenmiştir. Hartmann sayısının pertürbe edilmiş üst duvara sahip kesit içerisindeki etkisini net olarak gözlemleyebilmek için öncelikle farklı Hartmann sayı değerleri için düzgün sınırlara sahip kesit problemi incelenmiş daha sonra pertürbe edilmiş yüzeye sahip problem için aynı Hartmann değerleri incelenmiştir. Görülmüştür ki küçük Hartmann değerleri için hız pertürbe edilmiş yüzeyli problemde daha küçük iken Hartmann değeri arttıkça aradaki fark yok olmuştur. İndüklenmiş manyetik alan ise pertürbe edilmiş yüzeyli problemde tüm Hartmann değerleri için daha büyük çıkmıştır. Son olarak, karşılıklı sınır elemanları metodu ile konveksiyon-difüzyon temel çözümleri kullanılarak düzgün yüzeye ve pertürbe edilmiş yüzeye sahip magnetohidrodinamik problemi çözülmüştür. Farklı Hartmann değerleri için yapılan incelemede bölge integrali içeren sınır değer problemi ile benzer sonuçlar elde edilmiştir.

Projenin öneri aşamasında:

**İlk altı aylık dönemde:** zamana bağlı magnetohidrodinamik probleminin pertürbe edilmiş yüzeye sahip dikdörtgen kesitli kanalda değişik iletkenlik koşulları için bölge integrali içeren sınır elemanları yöntemi ile farklı temel çözümlerin kullanıldığı durumlar için bilgisayar kodu yazılacağı ve elde edilen sonuçların grafiksel olarak sunulacağı

**İkinci altı aylık dönemde:** aynı problem için karşılıklı sınır elemanları yöntemi tanımlanarak ilgili bilgisayar kodunun yazılacağı ve her iki metot ile elde edilen sonuçların karşılaştırılması olarak verileceği

taahhüt edilmişti. Yapılan çalışmalar sonucu proje önerisinde belirtilen taahhütlerin tümü yerine getirilmiş olup elde edilen sonuçlar ayrıntılı olarak incelenip yorumlanmıştır. Proje çıktısı olarak yayınlanan makalemizde proje konusu, literatür taraması, kullanılan metotlar ve probleme uygulamaları, ve elde edilen sonuçlar ayrıntılı olarak verilmiştir. Makalemiz bu rapora eklenmiştir.

## YAYINLAR/BİLDİRİLER

1. MHD flow in a rectangular duct with a perturbed boundary” başlıklı çalışma 26-28 Haziran 2018 tarihinde Paris, Fransa’ da düzenlenen IABEM 2018 Uluslararası Konferansı’nda sunulmuş ve özet kitapçığında basılmıştır.

Fendoglu, H., Bozkaya, C. and Tezer-Sezgin, M. (2018). *MHD flow in a rectangular duct with a perturbed boundary*. Symposiom of the International Association for Boundary Element Methods-IABEM 2018, Paris, France (June 26-28), p.44.

2. “MHD flow in a rectangular duct with a perturbed boundary” başlıklı makale “Computers and Mathematics with Applications” isimli dergide basılmıştır.

Fendoglu, H., Bozkaya, C. and Tezer, M. (2019). MHD flow in a rectangular duct with a perturbed boundary. *Computers and Mathematics with Applications*, 77, 374-388.

**NOT:** Bu yayınlar ekler bölümünde verilmiştir.

## **EKLER**

**MHD flow in a rectangular duct with a perturbed boundary****Hande Fendoglu<sup>1,\*</sup>, Canan Bozkaya<sup>1</sup>, Munevver Tezer-Sezgin<sup>1</sup>**<sup>1</sup>Department of Mathematics, Middle East Technical University, Ankara, Turkey

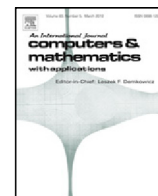
\*Email: hande.fendoglu@metu.edu.tr

**Keywords:** DBEM, MHD flow, Perturbed boundary

In this paper, a numerical study is carried for solving the unsteady magnetohydrodynamic (MHD) flow of a viscous, incompressible and electrically conducting fluid in a rectangular duct with a perturbed boundary subjected to an external magnetic field applied in y-direction. A small boundary perturbation of magnitude  $\epsilon$  is applied on the upper wall of the duct which is encountered in the visualization of the vein anatomy and blood flow in constricted arteries. The governing MHD flow convection-diffusion type equations are coupled in the velocity and the induced magnetic field. No-slip conditions are assumed on the boundary of the duct in which the vertical walls are insulated and the horizontal walls are perfectly conducting. The numerical method is based on the use of the domain boundary element method (DBEM) in spatial discretization and a backward finite difference scheme is employed in time integration. These MHD equations are decoupled first into two transient convection-diffusion equations, and then into two modified Helmholtz equations by using suitable transformations. Then, DBEM is used to transform these equations into equivalent integral equations by employing the fundamental solution of either steady-state convection-diffusion or modified Helmholtz equations. Thus, the resulting BEM integral equations contain a domain integral whose kernel involves the multiplication of the fundamental solution with the first order time derivative of the unknown, and it is treated by numerical integration. The velocity and the induced magnetic fields are visualized in terms of equi-velocity and current lines at transient and steady-state levels for several values of Hartmann number and the boundary perturbation parameter. The validity of the code is ascertained by comparing the obtained results with the ones given in literature [2]. The results reveal that the well-known characteristics of MHD flow are captured, that is, as  $M$  increases the velocity decreases and becomes stagnant at the center of the duct and a boundary layer formation is observed for both the velocity and the induced magnetic field. The perturbation parameter and the shape of the curved boundary significantly affect the behavior of the flow and cause an increase in the magnitude of induced magnetic field. DBEM with the fundamental solution of convection-diffusion equation gives better results compared to the ones obtained with the fundamental solution of modified Helmholtz equation in the sense of increasing  $M$ .

**References**

- [1] Dragos, L., *Magneto-Fluid Dynamics*. Abacus Press, England, 1975.
- [2] U. S. Mahabaleshwar, I. Pazanin, M. Radulovic, F. J. Suarez-Grau, *Effects of small boundary perturbation on the MHD duct flow*. Theoretical and Applied Mechanics, 44, 83-101, 2017.
- [3] C.L.N. Cunha, J.A.M. Carrer, M.F. Oliveira, V.L. Costa, *A study concerning the solution of advection-diffusion problems by the boundary element method*. Engineering Analysis with Boundary Elements, 65, 79-94, 2016.



# MHD flow in a rectangular duct with a perturbed boundary

Hande Fendoğlu, Canan Bozkaya\*, Münevver Tezer-Sezgin

Department of Mathematics of Middle East Technical University, 06800, Cankaya, Ankara, Turkey



## ARTICLE INFO

### Article history:

Received 29 May 2018

Received in revised form 8 September 2018

Accepted 22 September 2018

Available online 25 October 2018

### Keywords:

DBEM

DRBEM

MHD flow

Boundary perturbation

## ABSTRACT

The unsteady magnetohydrodynamic (MHD) flow of a viscous, incompressible and electrically conducting fluid in a rectangular duct with a perturbed boundary, is investigated. A small boundary perturbation  $\varepsilon$  is applied on the upper wall of the duct which is encountered in the visualization of the blood flow in constricted arteries. The MHD equations which are coupled in the velocity and the induced magnetic field are solved with no-slip velocity conditions and by taking the side walls as insulated and the Hartmann walls as perfectly conducting. Both the domain boundary element method (DBEM) and the dual reciprocity boundary element method (DRBEM) are used in spatial discretization with a backward finite difference scheme for the time integration. These MHD equations are decoupled first into two transient convection–diffusion equations, and then into two modified Helmholtz equations by using suitable transformations. Then, the DBEM or DRBEM is used to transform these equations into equivalent integral equations by employing the fundamental solution of either steady-state convection–diffusion or modified Helmholtz equations. The DBEM and DRBEM results are presented and compared by equi-velocity and current lines at steady-state for several values of Hartmann number and the boundary perturbation parameter.

© 2018 Elsevier Ltd. All rights reserved.

## 1. Introduction

Magnetohydrodynamics (MHD) studies the motion of electrically conducting fluids in the presence of magnetic fields. The magnetic field influences the fluid motion which is expressed mathematically by including the electromagnetic force in the equations of motion. The interaction between the external magnetic field and fluid motion gives rise to induced magnetic field through Ohm's law. The governing equations of MHD flow are the Navier–Stokes equations of fluid dynamics and Maxwell's equations of electromagnetism. MHD has wide range of engineering applications such as MHD generators, pumps, accelerators, blood flow measurements, power generation, geothermal energy extraction, producing liquid metals, nuclear fusion. Coupling of these equations, however, leaves analytical solutions available for only simple cases [1–3]. Therefore it is important to develop efficient numerical techniques to obtain approximate solutions for the MHD flow problems.

Many researchers have investigated the MHD flow problem using several numerical methods. Steady flows have been studied widely compared to the transient MHD flows in regular domains like rectangular/triangular ducts with straight boundaries (e.g. [4–6]) and in complex geometries like annular-like domains in [7]. However, here we will focus on only the papers that provide solution to time-dependent MHD flows. The unsteady MHD flow equations have been studied using the finite element method (FEM) in two-dimensional rectangular, circular and triangular pipes by Singh and Lal [8]. They observed that when the wall conductivity and Hartmann number increase, the flux through a section is reduced and the steady-state is approached at a faster rate. Salah et al. [9] developed a solution algorithm for the three-dimensional

\* Corresponding author.

E-mail address: [bcanan@metu.edu.tr](mailto:bcanan@metu.edu.tr) (C. Bozkaya).

coupled MHD flow. This method is valid for both high and low magnetic Reynolds numbers. Seungsoo and Dulikravich [10] gave a finite difference method (FDM) for three-dimensional unsteady MHD flow in a rectangular channel along with a temperature variation. Additionally, Sheu and Lin [11] proposed convection–diffusion–reaction model for solving unsteady MHD flow with a FDM on non-staggered grids using a transport scheme in each ADI spatial sweep. Their results are in good agreement with the analytical solutions and show high rate of convergence. Some meshless methods have also been proposed for solving MHD flow equations in channels of different cross-sections and for arbitrary wall conductivities. Dehghan and Mirzaei [12,13], and Loukopoulos et al. [14], presented meshless local boundary integral equation method, meshless Local Petrov Galerkin method and localized meshless point collocation method, respectively, for solving unsteady MHD flow equations. A numerical scheme which is a combination of the dual reciprocity BEM (DRBEM) for space and the differential quadrature method (DQM) for the time discretization, is proposed by Bozkaya and Tezer-Sezgin [15] for the solution of unsteady MHD flow problem in a regular rectangular duct with insulated walls. Thus, the solution was obtained at any required time level without the need of step-by-step computation with respect to time. For the unsteady MHD flow in a duct with arbitrary wall conductivity, the BEM formulation with time-dependent fundamental solution is presented by Bozkaya and Tezer-Sezgin [16] and the numerical solutions are obtained for higher values of Hartmann numbers compared to previous studies.

Concerning the solution of the unsteady MHD flow equations, two BEM formulations namely DBEM and DRBEM are presented in this paper. The use of the DBEM with different fundamental solutions as a tool for the solution of the MHD flow equations is the main contribution of this paper. The time-dependent MHD flow in a rectangular duct with a perturbed boundary subject to an external magnetic field is considered as a physically challenging problem but studied very rarely. The effect of boundary perturbation on the fluid flow has been given in the work of Mahabaleshwar et al. [17] and for the steady MHD flow, in the study of Marušić-Paloka and Pažanin [18] for the Darcy–Brinkman flow and for incompressible viscous flow by Jäger [19]. In the work of Aydın and Tezer-Sezgin [20], the MHD flow direct and Cauchy problems in a rectangular duct with a perturbed slipping upper boundary are solved asymptotically by the use of dual reciprocity BEM to recover the slip length on the perturbed boundary through the slip boundary conditions for relatively small values of Hartmann number. Thus, a small boundary perturbation of magnitude  $\varepsilon$  is applied on the upper Hartmann wall of the duct in the present study. The walls parallel to applied magnetic field (side walls) are taken to be insulated while the perpendicular walls (Hartmann walls) are perfectly conducting with the assumption of no-slip velocity conditions on the duct walls. The convection–diffusion type coupled MHD equations are decoupled first into two transient convection–diffusion equations but it makes the boundary conditions coupled (for perfectly conducting walls). Then, by using exponential type transformations, these convection–diffusion equations are transformed into two modified Helmholtz equations. The DBEM is then used to transform these equations into equivalent integral equations by employing the fundamental solution of either steady-state convection–diffusion or modified Helmholtz equations, respectively. It is observed that the DBEM with the fundamental solution of convection–diffusion equation gives more accurate results compared to the use of fundamental solution of modified Helmholtz equation. The DRBEM technique is also performed to solve the transient MHD flow equations by using fundamental solution of convection–diffusion equation and the results are compared with the ones obtained by DBEM. The difference between the applications of DBEM and DRBEM is the treatment of the leftover domain integral due to the time derivative term. That is, the domain integral is kept and evaluated by numerical integration in DBEM while in DRBEM it is transformed into an equivalent integral defined only on the boundary of the duct. The effect of the perturbed upper boundary on the velocity and induced magnetic field is studied in detail. The results are presented by equivelocity and current lines for several values of Hartmann number, the boundary perturbation parameters and the boundary perturbation functions.

## 2. The mathematical formulation of the problem

The unsteady MHD flow equations which are coupled in the velocity  $V(x, y)$  and induced magnetic field  $B(x, y)$ , are given in non-dimensional form as [1]

$$\nabla^2 V + M \frac{\partial B}{\partial y} = -1 + \frac{\partial V}{\partial t} \quad \text{in } \Omega \quad (1)$$

$$\nabla^2 B + M \frac{\partial V}{\partial y} = \frac{\partial B}{\partial t}$$

with the no-slip velocity boundary conditions  $V = 0$  on  $\Gamma$  (boundary of the domain  $\Omega$ ). The side walls are taken to be insulated ( $B = 0$ ), while the Hartmann walls are perfectly conducting ( $\frac{\partial B}{\partial n} = 0$ ). Here, Hartmann number  $M$  is defined by  $M = B_0 L_0 \sqrt{\sigma} / \sqrt{\mu}$ , where  $L_0$  is the characteristic length,  $B_0$  is the intensity of the applied magnetic field,  $\sigma$  and  $\mu$  are the electrical conductivity and the coefficient of viscosity of the fluid, respectively. The upper wall of the duct is perturbed as shown in Fig. 1, [17]. Thus, the duct domain  $\Omega$  is

$$\Omega = \{(x, y) \in \mathbb{R}^2 : -c < x < c, -1 < y < 1 - \varepsilon f(x)\} \quad (2)$$

where  $\varepsilon$  is the perturbation parameter arbitrarily small ( $0 < \varepsilon \ll 1$ ), while  $f$  is assumed to be an arbitrary smooth perturbation function and  $c$  is a constant.

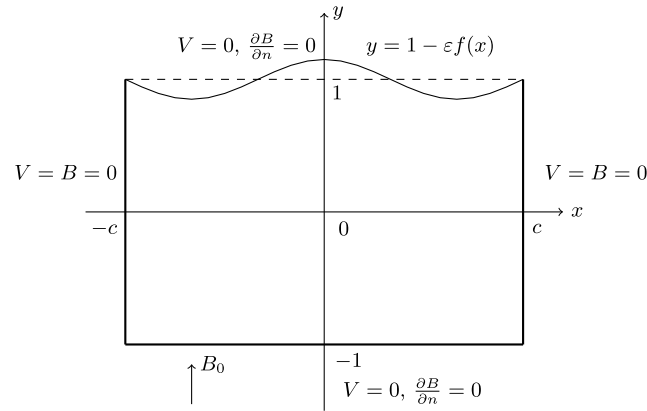


Fig. 1. Cross-section of a perturbed duct with boundary conditions.

Eqs. (1) are decoupled into two convection–diffusion equations given as

$$\nabla^2 w_1 + M \frac{\partial w_1}{\partial y} = -1 + \frac{\partial w_1}{\partial t} \tag{3}$$

in  $\Omega$

$$\nabla^2 w_2 - M \frac{\partial w_2}{\partial y} = -1 + \frac{\partial w_2}{\partial t} \tag{4}$$

by defining  $w_1 = V + B$  and  $w_2 = V - B$ . Then, the corresponding boundary conditions become

$$\text{For insulated walls : } w_1 = 0, \quad w_2 = 0, \tag{5}$$

$$\text{For perfectly conducting walls : } w_2 = -w_1, \quad \frac{\partial w_2}{\partial n} = \frac{\partial w_1}{\partial n}.$$

The resulting convection–diffusion equations (3)–(4) can be further transformed into two transient modified Helmholtz equations

$$\nabla^2 u_1 - \frac{M^2}{4} u_1 = -\exp\left(\frac{M}{2} r_y\right) + \frac{\partial u_1}{\partial t} \tag{6}$$

in  $\Omega$

$$\nabla^2 u_2 - \frac{M^2}{4} u_2 = -\exp\left(-\frac{M}{2} r_y\right) + \frac{\partial u_2}{\partial t} \tag{7}$$

by using the exponential type transformation  $u_1 = \exp\left(\frac{M}{2} r_y\right) w_1$  and  $u_2 = \exp\left(-\frac{M}{2} r_y\right) w_2$ . Here,  $r$  is the magnitude of the position vector  $\vec{r} = (r_x, r_y)$  between the source and field points. The corresponding boundary conditions are

$$\text{For insulated walls : } u_1 = 0, \quad u_2 = 0, \tag{8}$$

$$\text{For perfectly conducting walls : } u_2 = -\exp(-Mr_y)u_1, \quad \frac{\partial u_2}{\partial n} = \exp(-Mr_y) \frac{\partial u_1}{\partial n}.$$

It is noticed that, while the original MHD equations (1) are decoupled as transient convection–diffusion equations (3)–(4) or modified Helmholtz equations (6)–(7) the corresponding boundary conditions are coupled as given in Eqs. (5) and (8), respectively. The original unknowns  $V$  and  $B$  can be obtained by using back substitutions

$$V = \frac{1}{2}(w_1 + w_2), \quad B = \frac{1}{2}(w_1 - w_2) \tag{9}$$

for the system of convection–diffusion type equations (3)–(4) and

$$V = \frac{1}{2}[\exp\left(-\frac{M}{2} r_y\right)u_1 + \exp\left(\frac{M}{2} r_y\right)u_2], \tag{10}$$

$$B = \frac{1}{2}[\exp\left(-\frac{M}{2} r_y\right)u_1 - \exp\left(\frac{M}{2} r_y\right)u_2]$$

for the system of modified Helmholtz equations (6)–(7).

### 3. Numerical methods

The unsteady MHD flow in a duct with a perturbed upper boundary will be solved numerically by the use of two types of boundary elements method, namely domain BEM and dual reciprocity BEM for the spatial discretization where a backward finite difference scheme is employed in time integration. Both techniques aim to transform the given differential equations into equivalent integral equations, which contain a domain integral due to the time derivative, by weighting the equations with the fundamental solution of the steady convection–diffusion or modified Helmholtz equations. The leftover domain integral is treated by numerical integration in DBEM while it is further transformed into a boundary integral by means of radial basis functions in DRBEM as mentioned before. Finally, the resulting DBEM and DRBEM system of first order time-dependent differential equations is discretized by the use of backward finite difference scheme.

#### 3.1. DBEM formulation

##### 3.1.1. DBEM formulation by using the fundamental solution of convection–diffusion equation

The DBEM is employed to transform the system (3)–(4) into equivalent integral equations by using the fundamental solution of convection–diffusion equation

$$u^* = u_{1,2}^* = \frac{1}{2\pi} \exp(\pm \frac{M}{2} r_y) K_0(sr) \tag{11}$$

where  $u_1^*$  and  $u_2^*$  are fundamental solutions of Eqs. (3) and (4), respectively. Here,  $K_0(sr)$  is the modified Bessel function of the second kind and of order zero, and  $s = \frac{M}{2}$ . The signs  $\pm$  in Eq. (11) are taken according to the signs given in Eqs. (3)–(4). The normal derivatives of  $u_1^*$  and  $u_2^*$  are  $q_1^*$  and  $q_2^*$ , respectively, and are given by

$$q^* = q_{1,2}^* = \frac{1}{2\pi} \exp(\pm \frac{M}{2} r_y) \left[ -sK_1(sr) \frac{\partial r}{\partial n} \pm \frac{1}{2} Mn_y K_0(sr) \right] \tag{12}$$

where  $\frac{\partial r}{\partial n}$  is the derivative of  $r$  in the direction of outward normal vector  $\vec{n} = (n_x, n_y)$  to the boundary  $\Gamma$ , and  $K_1(sr)$  is the modified Bessel function of the second kind and of order one. Weighting Eqs. (3) and (4) with  $u_1^*$  and  $u_2^*$ , respectively, and applying the Green’s second identity two times [21], one gets

$$c_i w_i + \int_{\Gamma} (q^* w - u^* \frac{\partial w}{\partial n}) d\Gamma \mp \int_{\Gamma} Mn_y u^* w d\Gamma = - \int_{\Omega} (\frac{\partial w}{\partial t} - 1) u^* d\Omega \tag{13}$$

where  $w$  denotes  $w_1$  and  $w_2$ ,  $u^*$  and  $q^*$  denote  $u_1^*$ ,  $u_2^*$  and  $q_1^*$ ,  $q_2^*$ , respectively. Here, the coefficient  $c_i$  ( $= \frac{\theta_i}{2\pi}$ ) is a constant where  $\theta_i$  being the internal angle at the source point  $i$ . The domain integrals on the right hand side of Eq. (13) will be kept in the integral equation and computed numerically [22]. When the boundary of the duct is discretized by using constant boundary elements, Eq. (13) can be stated as

$$Hw - G \frac{\partial w}{\partial n} = - \int_{\Omega} u^* \frac{\partial w}{\partial t} d\Omega + \int_{\Omega} u^* d\Omega. \tag{14}$$

The components of  $H$  and  $G$  matrices are,

$$H_{ij} = c_i \delta_{ij} + \frac{1}{2\pi} \int_{\Gamma_j} \exp(\pm \frac{M}{2} r_y) \left[ -sK_1(sr) \frac{\partial r}{\partial n} \mp \frac{Mn_y}{2} K_0(sr) \right] d\Gamma_j \tag{15}$$

$$G_{ij} = \frac{1}{2\pi} \int_{\Gamma_j} \exp(\pm \frac{M}{2} r_y) K_0(sr) d\Gamma_j \tag{16}$$

and the diagonal entries of  $H$  and  $G$  are calculated analytically as

$$H_{ii} \approx c_i \mp \frac{Mn_y l}{4\pi} (\ln \frac{2}{l} + 1 - \ln \frac{s}{2} - \gamma) \tag{17}$$

$$G_{ii} \approx \frac{l}{2\pi} (\ln \frac{2}{l} + 1 - \ln \frac{s}{2} - \gamma) \tag{18}$$

where  $l$  is the length of element,  $\gamma$  is Euler constant and  $\delta$  is Kronecker delta function.

Further, the time derivative on the right hand side of Eqs. (14) is discretized by using implicit backward difference approximation

$$\frac{\partial w^{(k+1)}}{\partial t} \approx \frac{w^{(k+1)} - w^{(k)}}{\Delta t}. \tag{19}$$

Then, Eq. (14) can be expressed as

$$(H + \frac{1}{\Delta t} R) w^{(k+1)} - G \frac{\partial w^{(k+1)}}{\partial n} = \frac{1}{\Delta t} R_d w^{(k)} + R \tag{20}$$

where  $R_d$  is a diagonal matrix which is constructed by taking the components of the vector  $R = \int_{\Omega} u^* d\Omega$  as its diagonal entries at each node and  $k$  denotes the time level. The domain integral is computed numerically by using numerical integration technique. The insertion of boundary conditions results in a system of linear equations,  $Az = b$ , where  $A$  is a full matrix with scattered zeros. Once the system is solved, the unknowns  $w_1, w_2$  and  $\frac{\partial w_1}{\partial n}, \frac{\partial w_2}{\partial n}$  are obtained on the boundary and in the interior according to given boundary conditions. Finally, the original unknowns  $V$  and  $B$  are obtained by using the back substitutions given in Eq. (9).

3.1.2. DBEM formulation by using the fundamental solution of modified Helmholtz equation

By applying the method of weighted residual [21] and employing the following fundamental solution of the modified Helmholtz equation

$$u^* = u_1^* = u_2^* = \frac{1}{2\pi} K_0(sr) \tag{21}$$

to the system (6)–(7), we obtain the following integral equation

$$c_i u_i + \int_{\Gamma} q^* u d\Gamma - \int_{\Gamma} u^* \frac{\partial u}{\partial n} d\Gamma = - \int_{\Omega} \frac{\partial u}{\partial t} u^* d\Omega + \int_{\Omega} \exp(\pm \frac{M}{2} r_y) u^* d\Omega. \tag{22}$$

Here,  $q^*$  is given as

$$q^* = q_1^* = q_2^* = - \frac{s}{2\pi} K_1(sr) \frac{\partial r}{\partial n} \tag{23}$$

where  $s = \frac{M}{2}$ . After the discretization of the boundary with constant elements, we obtain the matrix–vector equations

$$Hu - G \frac{\partial u}{\partial n} = - \int_{\Omega} u^* \frac{\partial u}{\partial t} d\Omega + \int_{\Omega} \exp(\pm \frac{M}{2} r_y) u^* d\Omega \tag{24}$$

which corresponds to the solutions  $u_1$  and  $u_2$  with + and – signs, respectively. The components of  $H, G$  are

$$H_{ij} = c_i \delta_{ij} - \frac{1}{2\pi} \int_{\Gamma_j} s K_1(sr) \frac{\partial r}{\partial n} d\Gamma_j, \quad G_{ij} = \frac{1}{2\pi} \int_{\Gamma_j} K_0(sr) d\Gamma_j \tag{25}$$

when  $i \neq j$ . The diagonal entries of the matrix  $H$  are directly equal to  $c_i$ , (i.e.  $H_{ii} = c_i$ ) since  $\frac{\partial r}{\partial n} = 0$  along a constant element in the integral (25) while the diagonal entries  $G_{ii}$  are calculated analytically using the formula (18).

The time derivative is again discretized by using implicit backward finite difference which results in

$$(H + \frac{1}{\Delta t} M_1) u^{(k+1)} - G \frac{\partial u}{\partial n}^{(k+1)} = \frac{1}{\Delta t} M_1 u^{(k)} + M_2 \tag{26}$$

where  $M_1$  is constructed as a diagonal matrix while  $M_2$  is a vector. At each node, the diagonal entries of  $M_1$  and entries of the vector  $M_2$  are computed as

$$M_1 = \int_{\Omega} u^* d\Omega, \quad M_2 = \int_{\Omega} \exp(\pm \frac{M}{2} r_y) u^* d\Omega \tag{27}$$

by using numerical integration technique as in Section 3.1.1. Insertion of boundary conditions results in a linear system to be solved iteratively for increasing time levels. To obtain the solution in original unknowns  $V$  and  $B$ , the back substitutions given in Eq. (10) are applied.

3.2. DRBEM formulation with the fundamental solution of convection–diffusion equation

Similar to DBEM when the fundamental solution of convection–diffusion equation is employed to Eqs. (3)–(4), we end up with the integral equation (13) which contains a domain integral involving the time derivative. The domain integral on the right hand side of Eq. (13) involving the nonhomogeneous terms is approximated by using the radial basis function  $f_j$  which is linked to the particular solution  $\hat{u}_j$  as  $\nabla^2 \hat{u}_j \pm M \frac{\partial \hat{u}_j}{\partial y} = f_j$ . Accordingly, this term is approximated by

$$\frac{\partial w}{\partial t} - 1 = \sum_{j=1}^{N+L} \alpha_j(t) f_j(x, y). \tag{28}$$

Substituting  $f_j$  into Eq. (28) and then into Eq. (13) gives

$$c_i w_i + \int_{\Gamma} (q^* w - u^* \frac{\partial w}{\partial n}) d\Gamma \mp \int_{\Gamma} M n_y u^* w d\Gamma = - \sum_{j=1}^{N+L} \alpha_j(t) \int_{\Omega} (\nabla^2 \hat{u}_j \pm M \frac{\partial \hat{u}_j}{\partial y}) u^* d\Omega \tag{29}$$

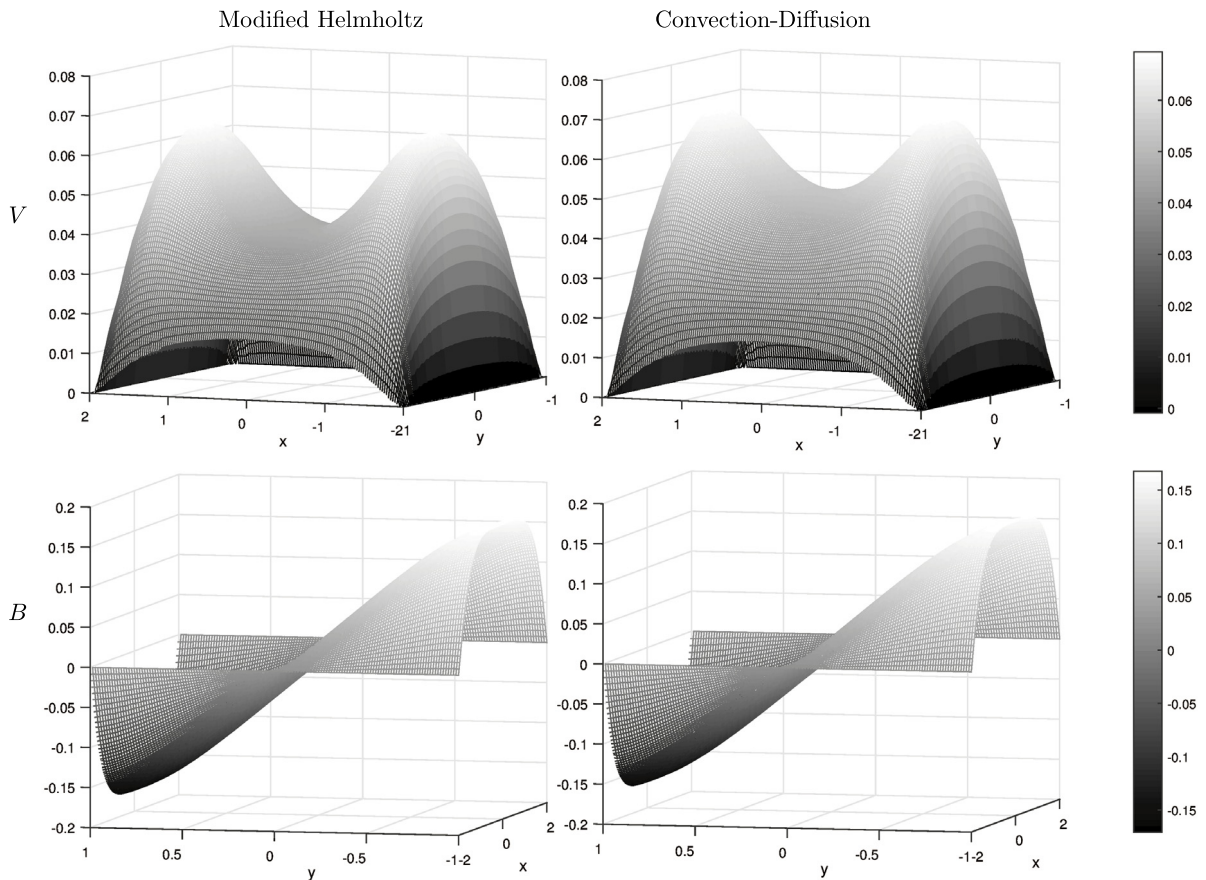


Fig. 2. The steady-state DBEM results with  $M = 5, \varepsilon = 0.1, f = -\cos(\frac{\pi x}{4})$ .

Applying Green’s second identity to the right hand side of Eq. (29) we obtain

$$c_i w_i + \int_{\Gamma} (q^* w - u^* \frac{\partial w}{\partial n}) d\Gamma \mp \int_{\Gamma} M n_y u^* w d\Gamma = \sum_{j=1}^{N+L} \alpha_j(t) \left[ c_i \hat{u}_{ji} + \int_{\Gamma} (q^* \hat{u}_j - u^* \hat{q}_j) d\Gamma \mp \int_{\Gamma} M n_y u^* \hat{u}_j d\Gamma \right] \tag{30}$$

which involves only the boundary integrals where  $\hat{q}_j = \frac{\partial \hat{u}_j}{\partial n}$  and  $\alpha_j(t)$  is a set of time dependent undetermined coefficients, and  $N$  and  $L$  are the number of constant boundary elements and arbitrarily selected interior nodes, respectively. Here, the radial basis functions are taken as  $f_j = (1+r_j) \pm (\frac{1}{2} + \frac{r_j}{3})(M r_y)$ . Then, the corresponding particular solutions become  $\hat{u}_j = \frac{r_j^2}{4} + \frac{r_j^3}{9}$  with normal derivatives are  $\hat{q}_j = (\frac{r_j}{2} + \frac{r_j^2}{3})(\frac{\partial r_j}{\partial n})$  [23]. The collocation of the right hand side of Eq. (13) at  $N + L$  points and substituting back into Eq. (30) give

$$H w - G \frac{\partial w}{\partial n} = (H \hat{U} - G \hat{Q}) F^{-1} (\frac{\partial w}{\partial t} - \bar{1}) \tag{31}$$

where  $F, \hat{U}, \hat{Q}$  are the  $(N + L) \times (N + L)$  matrices obtained by taking  $f_j, \hat{u}_j, \hat{q}_j$  as columns, respectively, [21] and  $\bar{1}$  is the vector of ones. The components of the matrices  $H$  and  $G$  and their diagonal entries are the same as given in Eqs. (15)–(18). When the time derivative is discretized by using the implicit backward difference, Eq. (31) becomes

$$(H + \frac{C}{\Delta t}) w^{(k+1)} - G \frac{\partial w^{(k+1)}}{\partial n} = \frac{C}{\Delta t} w^{(k)} + C \bar{1} \tag{32}$$

where  $C = -(H \hat{U} - G \hat{Q}) F^{-1}$ . The DRBEM discretized system (32) corresponds again to the solutions  $w_1$  and  $w_2$  in Eqs. (3) and (4), respectively. Insertion of boundary condition results in a linear system to be solved iteratively for increasing time levels. To obtain the solution in original variables  $V$  and  $B$ , the back substitutions given in Eq. (9) is applied as in the DBEM application.

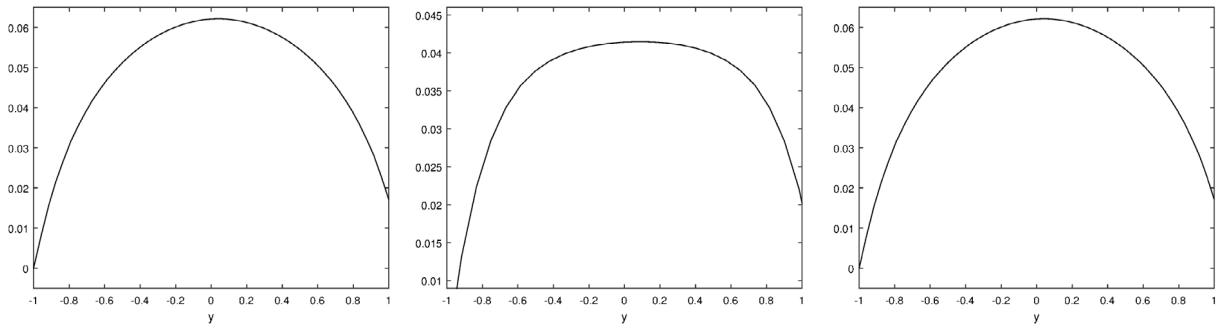


Fig. 3. Velocity profile along the vertical lines  $x = -1.0$  (left),  $x = 0$  (middle) and  $x = 1.0$  (right).

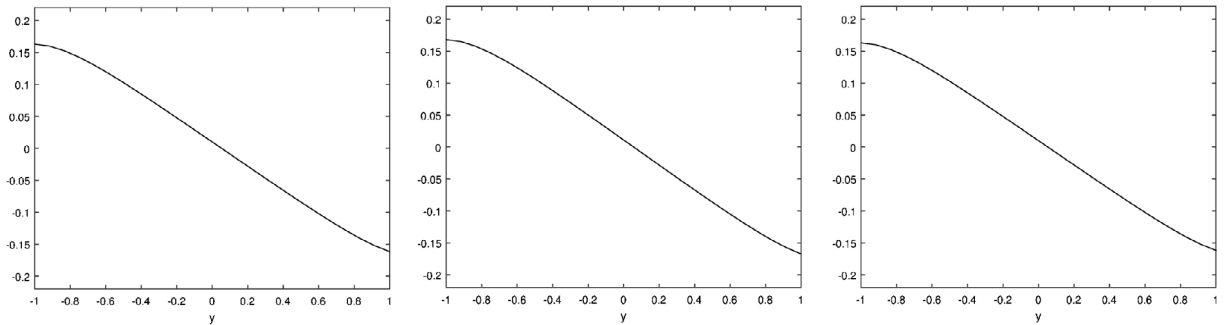


Fig. 4. Induced magnetic field profile along the vertical lines  $x = -1.0$  (left),  $x = 0$  (middle) and  $x = 1.0$  (right).

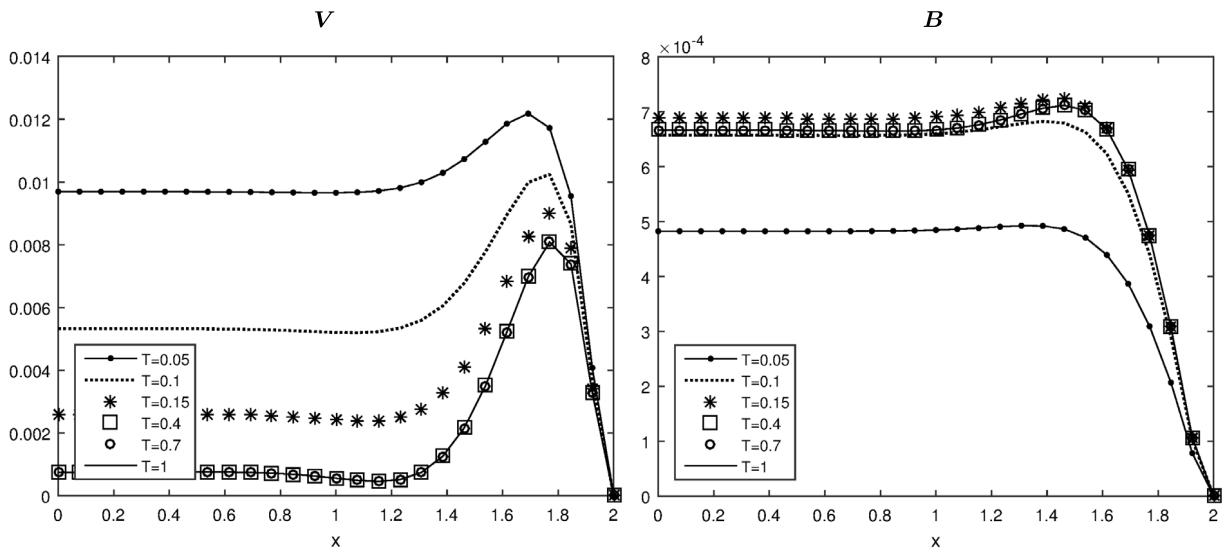


Fig. 5. Velocity and induced magnetic field along horizontal centerline  $y = 0$ ,  $M = 30$ ,  $\epsilon = 0$ .

### 4. Numerical results and discussions

The unsteady MHD flow equations are solved by both DBEM and DRBEM. DBEM application is given for two types of fundamental solutions, namely fundamental solution of modified Helmholtz and convection–diffusion equations. The numerical simulations of DBEM with fundamental solution of convection–diffusion equation are carried out for several values of perturbation parameter ( $\epsilon$ ) and Hartmann number ( $M$ ). Moreover, the effect of Hartmann number is presented elaborately for the MHD flow with flat walls and also for perturbed upper boundary. And then, DRBEM application with the fundamental solution of convection–diffusion equation is carried for the ducts with both flat and perturbed walls. Finally,

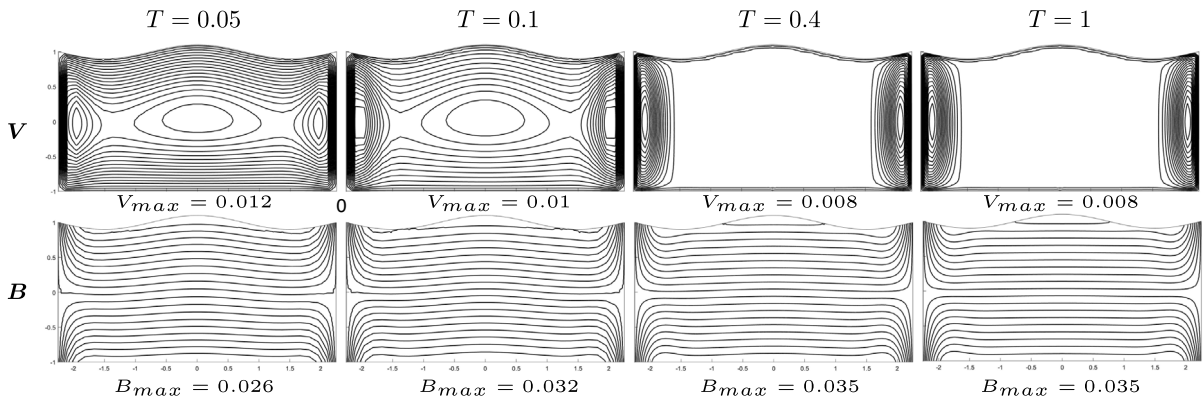


Fig. 6. Time evolutions of velocity and induced current for  $M = 30, f = -\cos(\frac{2\pi x}{3})$  and  $\varepsilon = 0.1$ .

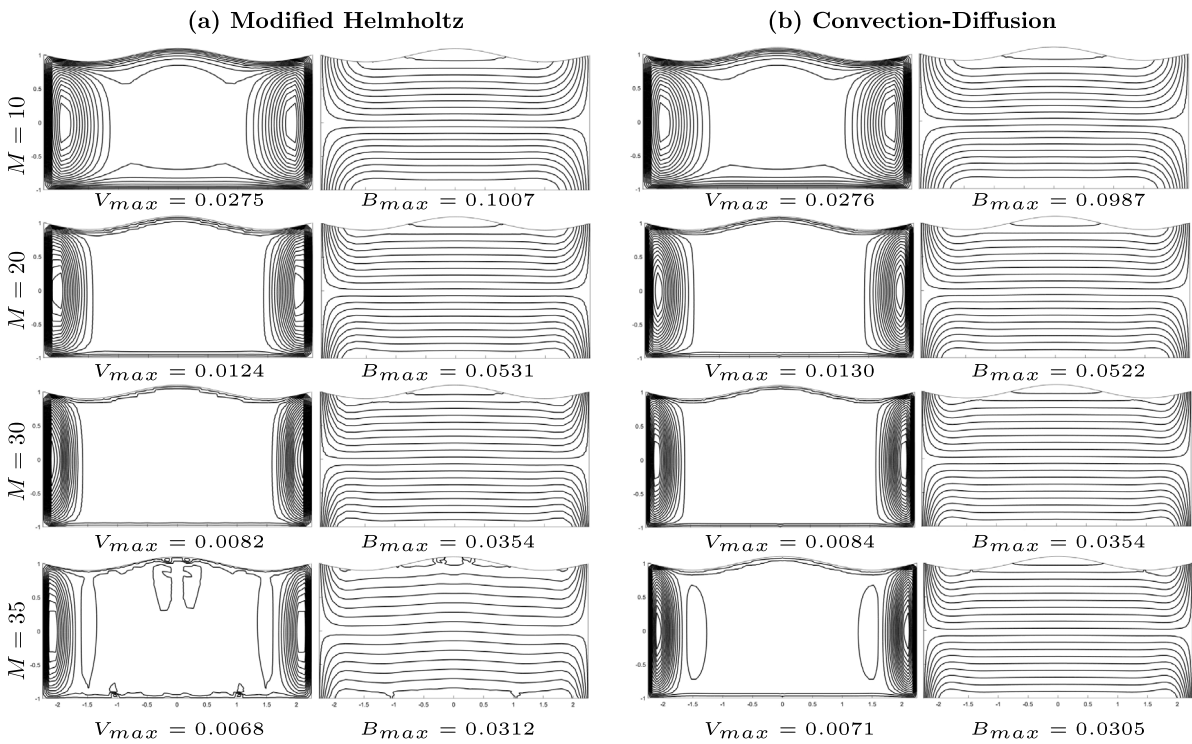


Fig. 7. Equivelocity and current lines by DBEM with the fundamental solution of (a) modified Helmholtz, (b) convection-diffusion equations for  $f = -\cos(\frac{2\pi x}{3}), \varepsilon = 0.1, T = 1$ .

the effect of perturbation function on the solution is investigated. For all computations, maximum  $N = 500$  and  $N = 1200$  constant boundary elements are used for the highest value of Hartmann number with DBEM and DRBEM, respectively.

The accuracy of the results obtained by DBEM either with the fundamental solution of modified Helmholtz or convection-diffusion equation is validated by comparing the obtained results with the ones given in the work [17] in terms of surface plots of velocity  $V$  and induced magnetic field  $B$  in Fig. 2. In this test problem, the perturbation function is taken as  $f = -\cos(\frac{\pi x}{4})$  for  $\varepsilon = 0.1$  and  $M = 5$ . The results are in well agreement with the results given in [17] (see Figure 14 and Figure 18 in [17]). Furthermore, for the same test problem the variation of the velocity and the induced magnetic field along the vertical lines  $x = \mp 1.0, 0$  are drawn in Figs. 3 and 4, respectively. The agreement of the present results with the ones given in [17] (see Figures 12,13,16,17 in [17]) is also well observed.

In the rest of the paper, we will focus on the effect of the perturbation function  $f (= -\cos(\frac{2\pi x}{3}))$  with several perturbation parameters ( $\varepsilon = 0, 0.1, 0.3, 0.5$ ) and Hartmann numbers ( $5 \leq M \leq 150$ ) on the flow and the induced magnetic field. In order to determine when the solution reaches to the steady-state, the velocity and induced magnetic field along the horizontal

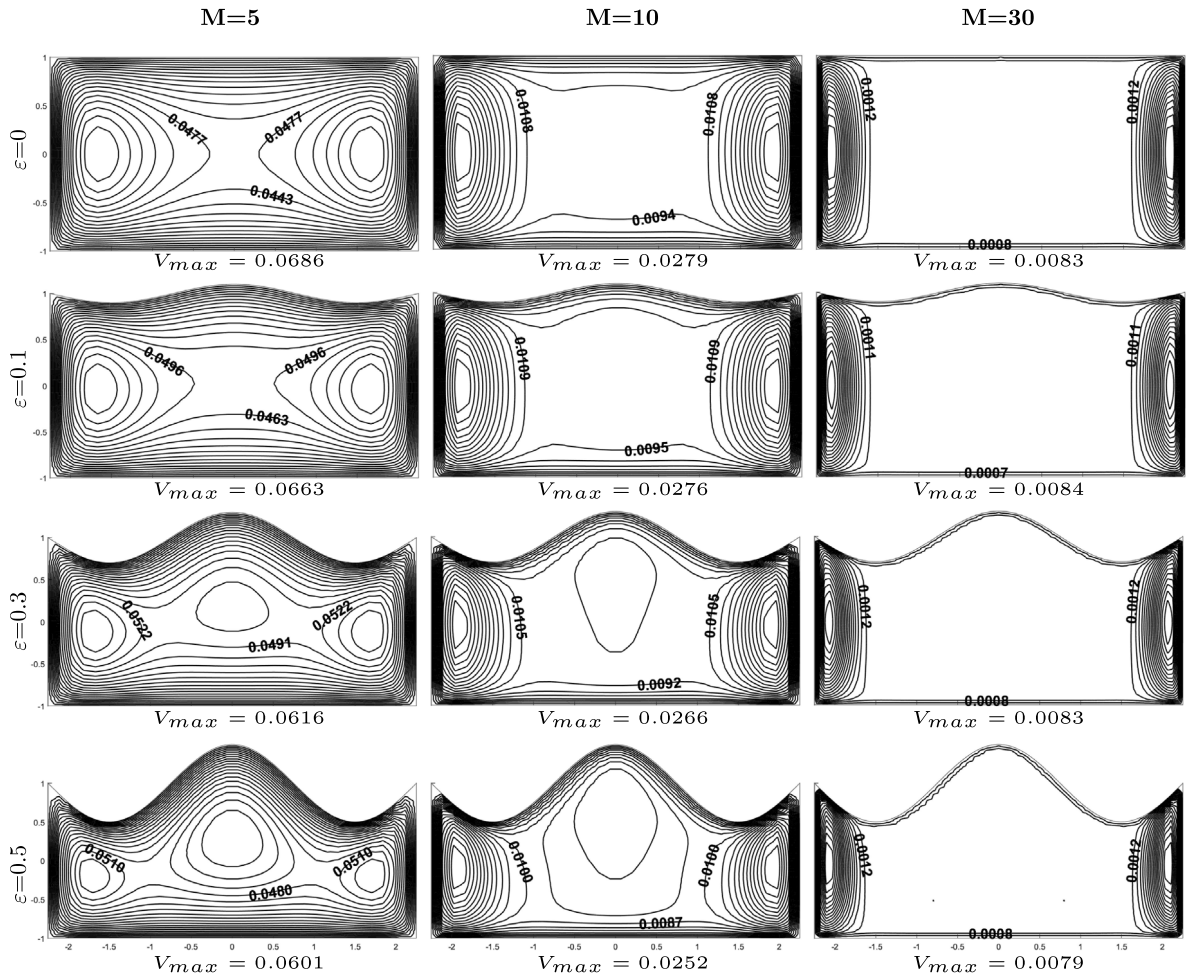


Fig. 8. The effect of  $\epsilon$  on the velocity with DBEM, when  $f = -\cos(\frac{2\pi x}{3})$ ,  $T = 1$ .

centerline ( $y = 0, 0 \leq x \leq 2$ ) are drawn in Fig. 5 at a fixed Hartmann number  $M = 30$  and  $\epsilon = 0$  at several time levels ( $0.05 \leq T \leq 1$ ). It is clear that, after  $T \geq 0.4$  the steady-state is reached for both the velocity and induced magnetic field.

Further, the DBEM solutions with the fundamental solution of convection–diffusion equation are illustrated in Fig. 6 for transient levels  $T = 0.05, 0.1, 0.4, 1$  when  $M = 30, f = -\cos(\frac{2\pi x}{3})$  and  $\epsilon = 0.1$ . Fig. 6 indicates that, solution reaches the steady-state when  $T \geq 0.4$ , which is quite compatible with Fig. 5. Thus, all the subsequent graphs are drawn at  $T = 1$  which is the steady-state level for both the velocity and the induced magnetic field.

First, we consider the effect of the use of different fundamental solutions in the application of DBEM on the velocity and induced magnetic field. Thus, the steady-state results obtained with the fundamental solution of modified Helmholtz and the convection–diffusion equations are compared in Fig. 7 in terms of velocity and induced magnetic field when  $M = 10, 20, 30, 35$  by taking  $f = -\cos(\frac{2\pi x}{3})$  with  $\epsilon = 0.1$ . For  $M \leq 30$ , both of the fundamental solutions provide the same results with a good accuracy. However, when  $M > 30$  DBEM with the fundamental solution of modified Helmholtz equation has difficulties in giving accurate results and some disruptions occur along the perturbed wall while the use of the fundamental solution of convection–diffusion results in acceptable results. Thus, the subsequent computations are performed by using DBEM with the fundamental solution of convection–diffusion equation.

The effect of the perturbation parameter  $\epsilon$  on the velocity and the induced magnetic field is displayed in Figs. 8 and 9, respectively. It is seen that the magnitude of the induced magnetic field increases with an increase in  $\epsilon$ , whereas there is a decrease in the velocity when  $M = 5, 10$ . When  $M = 30$  the increase rate in the magnitude of induced magnetic field becomes very small compared to the cases when  $M = 5, 10$ ; and there is almost no change in the velocity. Moreover, the fluid flows in terms of two eddies close to the side walls. It is well observed that at small values of Hartmann number ( $M = 5, 10$ ) an additional vortex is formed at the center of the cavity and this vortex moves upwards due to the expansion of the computational domain with an increase in  $\epsilon$ . A further increase in the Hartmann number results in a retardation in the fluid flow at the center of the cavity and the fluid flows completely in terms of two side layers weakening the effect of

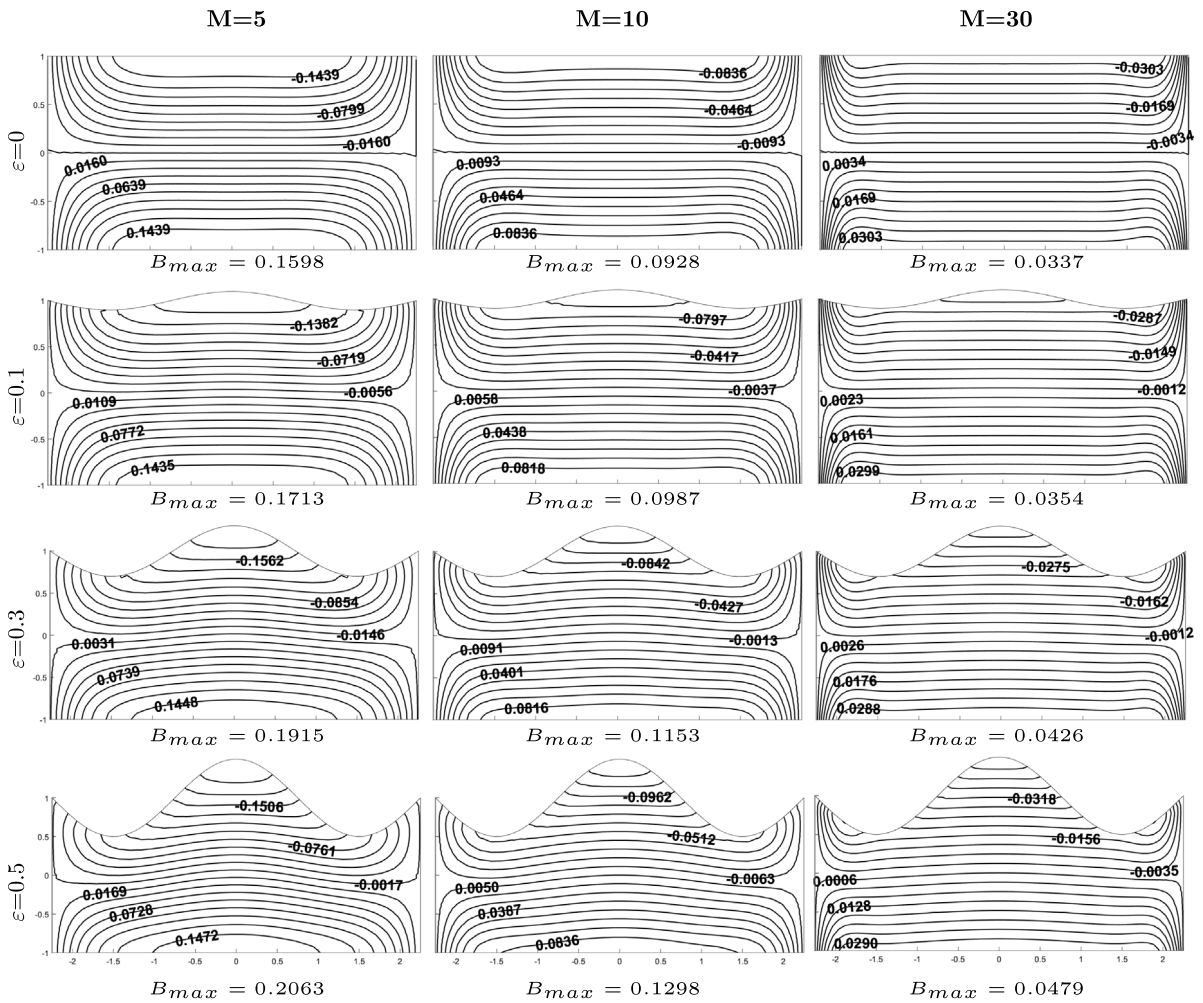


Fig. 9. The effect of  $\varepsilon$  on the induced magnetic field with DBEM when  $f = -\cos(\frac{2\pi x}{3})$ ,  $T = 1$ .

the perturbation. On the other hand, current lines fill the region due to the perturbed upper boundary obeying its boundary conditions, and start to form side layers as  $M$  increases.

Further, the effect of the Hartmann number on the velocity and the induced magnetic field is presented in Fig. 10 for a rectangular duct with flat walls and in Fig. 11 for a duct with perturbed upper wall ( $f = -\cos(\frac{2\pi x}{3})$ ), respectively. It is observed that, as  $M$  increases the flow is separated into two vortices near the side walls, the velocity drops and the fluid becomes stagnant at the center of the duct. Moreover, boundary layer formation is observed on the insulating parts of the boundary for both the velocity and the induced magnetic field as  $M$  increases. As Hartmann number increases to  $M = 50$ , Hartmann layers are developed for the flow, however, with a further increase in  $M$  to 150 the Hartmann layers are weakened and finally vanish. Side layers are also observed for the induced current lines for increasing  $M$ .

Moreover, the induced magnetic field is antisymmetric with respect to  $x$ -axis and the current lines are perpendicular to conducting walls as expected. The magnitude of the induced magnetic field increases for each Hartmann number when the upper wall of the duct is perturbed. On the other hand, a decrease in the velocity is well-observed for moderate values of  $M (\leq 50)$  in the perturbed duct when compared to the velocity in the duct with regular flat walls. This velocity drop is not seen for Hartmann number values  $M > 50$  since the flattening flow is the dominating case as  $M$  increases.

In addition, DRBEM is also employed to solve the unsteady MHD flow with perturbed boundary by using fundamental solution of convection–diffusion equation. The results are obtained for several values of Hartmann number, and are presented in Fig. 12, for rectangular duct both with flat walls and with a perturbed upper wall. The results that we obtain for rectangular duct with flat walls and with perturbed boundary (with  $f = -\cos(\frac{2\pi x}{3})$ ) are almost the same with our previous results based on DBEM. Maximum 900 boundary elements are used in DRBEM for highest value of Hartmann number, while 500 boundary elements are used in DBEM. Thus, DRBEM is in need of using more boundary elements than the DBEM to achieve accurate results which indicates that the DRBEM is computationally less efficient than DBEM as Hartmann number increases.

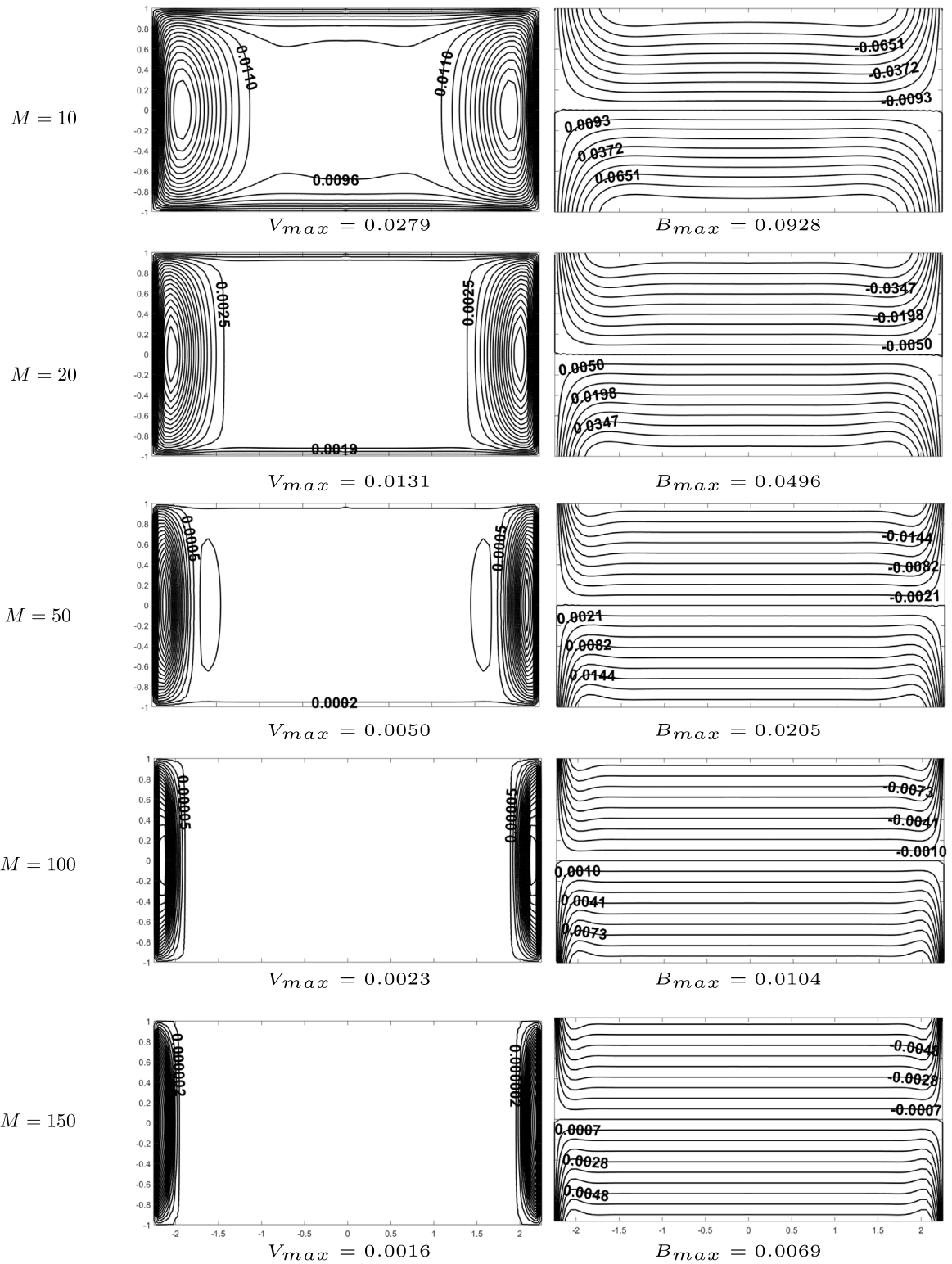
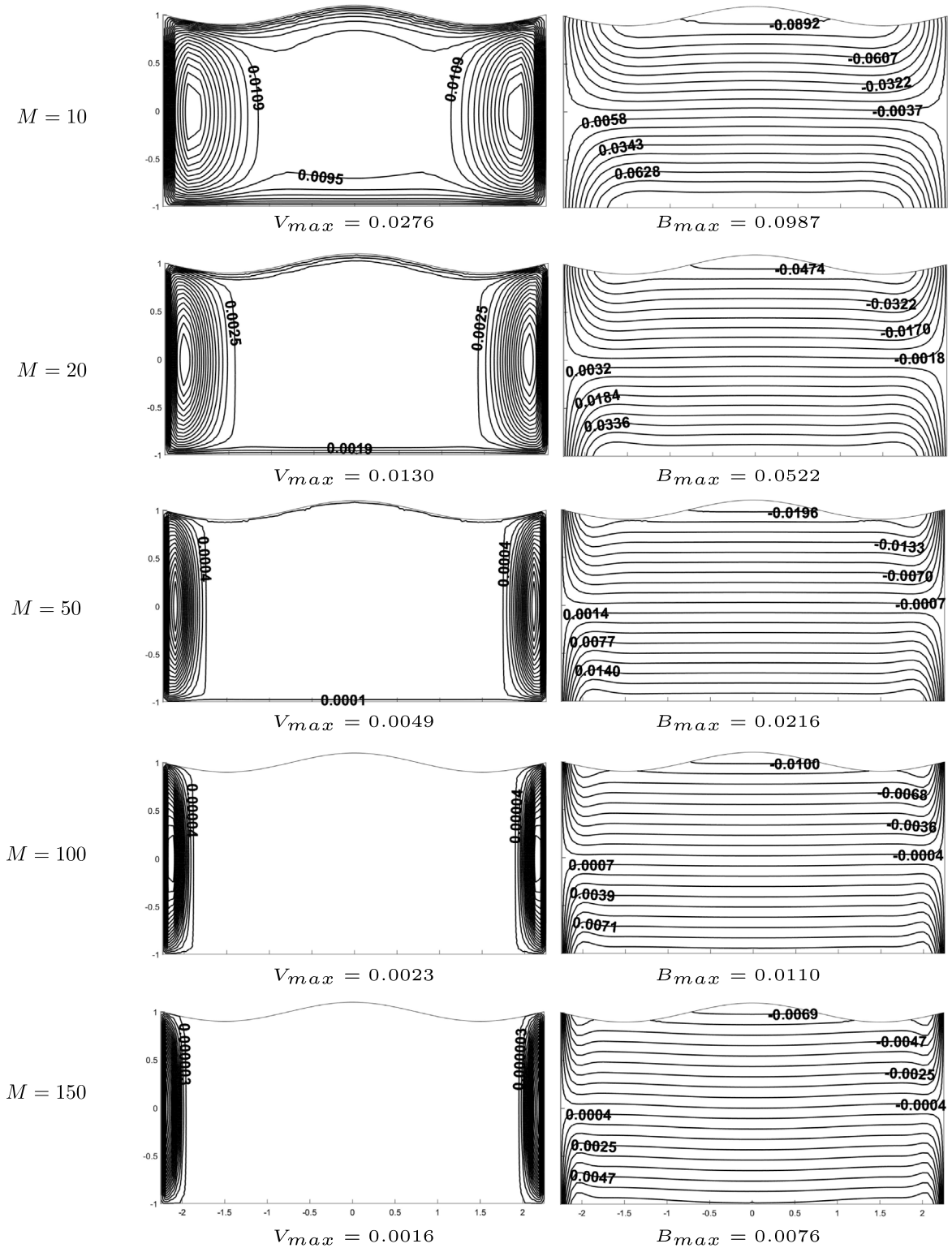


Fig. 10. Effect of  $M$  on equivalocity and current lines in a rectangular duct with flat walls (DBEM).

Finally, we obtain the solution of MHD duct flow in duct with a different shape of upper boundary which is determined by the perturbation function  $f$ . We consider basically two different shapes of upper wall, that is either concave down or concave



**Fig. 11.** Effect of  $M$  on equivelocity and current lines in a rectangular duct with perturbed upper wall when  $f = -\cos(\frac{2\pi x}{3})$ ,  $\varepsilon = 0.1$ ,  $T = 1$  (DBEM).

up around vertical centerline of the duct. Fig. 13 shows that the flow is divided into two vortices forming side layers and becoming stagnant at the center when the upper curve boundary is concave down at its middle part (for  $f = -\cos(\frac{\pi x}{4})$  and

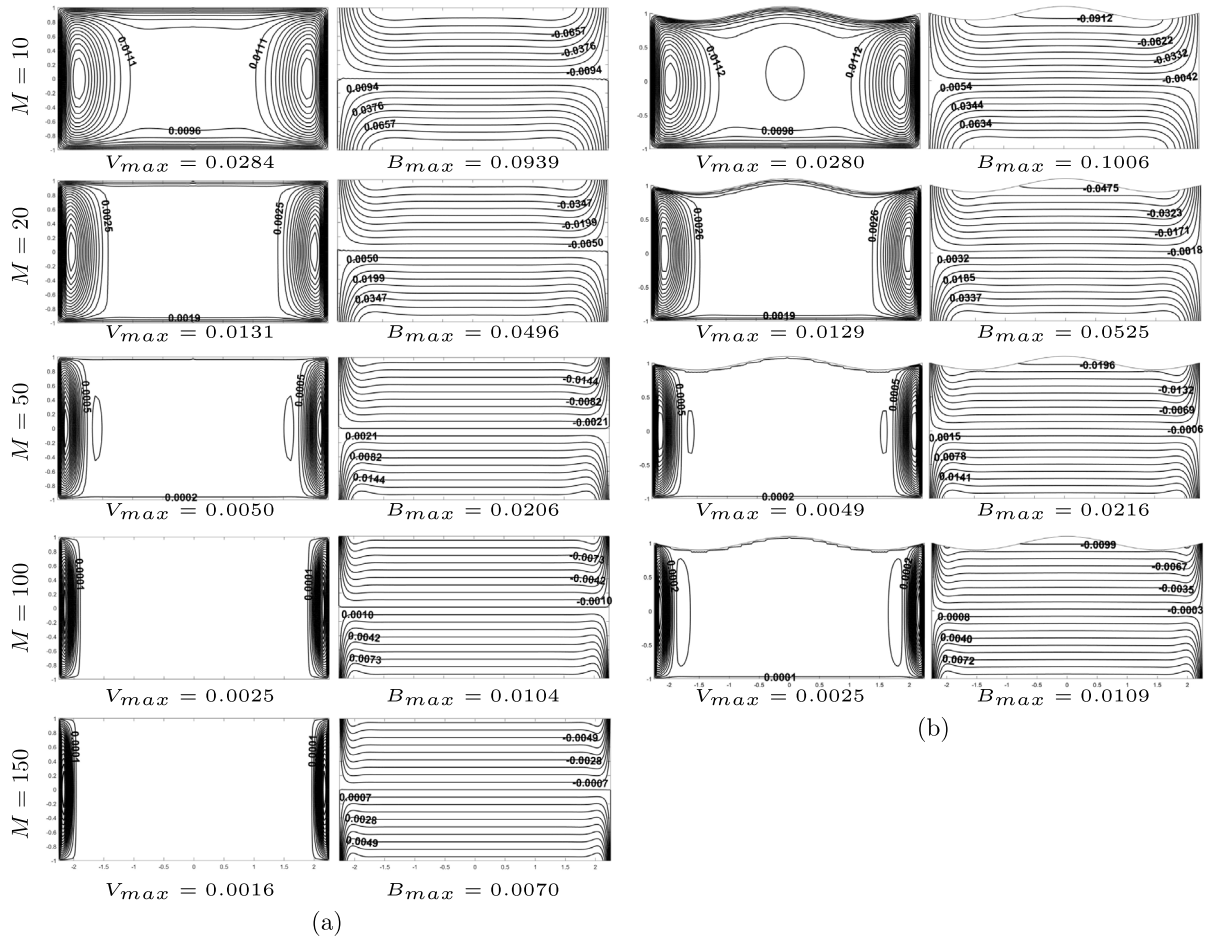


Fig. 12. Effect of  $M$  on the equivelocity and current lines in a duct with (a) flat walls, (b) a perturbed upper wall when  $f = -\cos(\frac{2\pi x}{3})$ ,  $\varepsilon = 0.1$  (DRBEM).

$f = -\cos(\frac{2\pi x}{3})$ ). On the other hand when the curved boundary is concave up (i.e.  $f = \cos(2\pi(1-x^2))$  and  $f = \sin(2\pi(1-x^2))$ ) at the middle part, the flow covers almost all the duct and the side layer formation is retarded. However, the induced magnetic field profiles are not altered much in both cases.

5. Conclusion

In this study, the transient MHD flow in a duct with a perturbed upper boundary is solved by DBEM and DRBEM when the vertical walls are insulated while the horizontal walls are perfectly conducting. It is observed that using DBEM with fundamental solution of convection–diffusion equation gives more accurate results compared to fundamental solution of modified Helmholtz equation. Therefore, only fundamental solution of convection–diffusion equation is employed in the application of DRBEM. An increase in the induced magnetic field is observed for each Hartmann number when the upper wall of the duct is perturbed while a decrease is seen in the velocity for moderate values of Hartmann number. The effect of perturbation parameter is well-observed in the velocity profile for small values of Hartmann number. That is, an additional vortex occurs at the center of the duct and moves towards the perturbed wall with an increase in  $\varepsilon$ . For the high values of Hartmann number no significant difference are observed due to the perturbed wall, since boundary layers are formed and the flow becomes stagnant at the center of the duct. The present results reveal that the well-known MHD flow characteristics are very well-captured with both the DBEM and DRBEM for the rectangular duct in flat walls. Moreover, for MHD flow with perturbed boundary, DBEM gives more accurate results compared to the DRBEM as Hartman number increases.

Acknowledgment

This work was supported by METU Project GAP-101-2018-2768, Turkey.

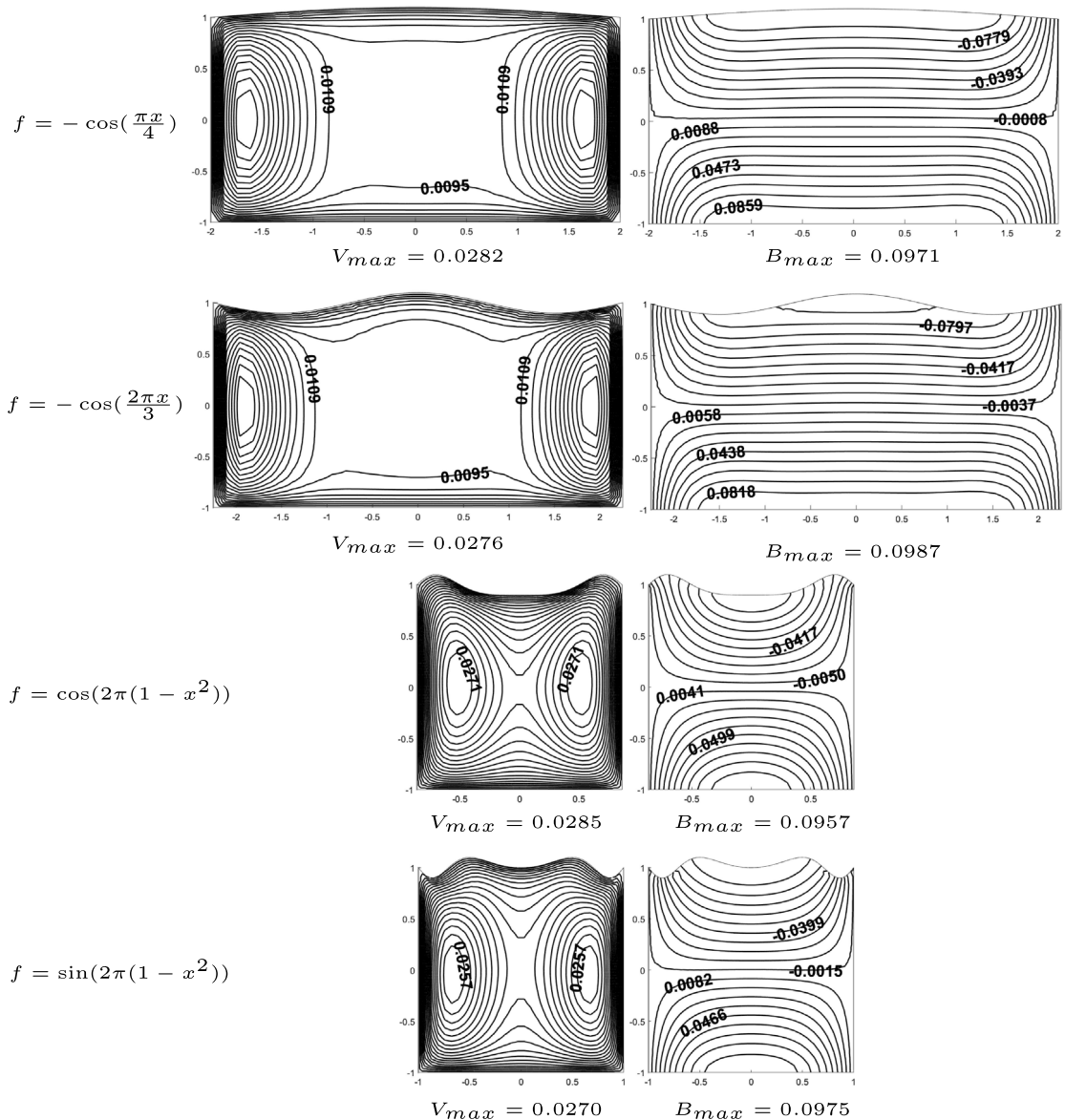


Fig. 13. The effect of perturbation function  $f$  on equivelocity and current lines at  $M = 10$ ,  $\varepsilon = 0.1$ ,  $T = 1$  (DBEM).

## References

- [1] L. Dragos, Magneto-Fluid Dynamics, Abacus Press, England, 1975.
- [2] J.A. Shercliff, A Textbook of Magnetohydrodynamics, Pergamon Press, Oxford-New York-Paris, 1965.
- [3] P.A. Davidson, An Introduction to Magnetohydrodynamics, Cambridge University Press, New York, 2001.
- [4] B. Singh, J. Lal, MHD axial flow in a triangular pipe under transverse magnetic field parallel to a side of the triangle, Indian J. Technol. 17 (1979) 184–189.
- [5] B. Singh, J. Lal, Finite element method of MHD channel flow with arbitrary wall conductivity, J. Math. Phys. Sci. 18 (1984) 501–516.
- [6] M. Tezer-Sezgin, S. Köksal, Finite element method for solving MHD flow in a rectangular duct, Internat. J. Numer. Methods Engrg. 28 (1989) 445–459.
- [7] C. Bozkaya, M. Tezer-Sezgin, Magnetohydrodynamic pipe flow in annular-like domains, Eur. J. Comput. Mech. 26 (2017) 394–410.
- [8] B. Singh, J. Lal, Finite element method for unsteady MHD flow through pipes with arbitrary wall conductivity, Int. J. Numer. Methods Fluids 4 (1984) 291–302.
- [9] N.B. Salah, A. Soulaïmani, W.G. Habashi, A finite element method for magnetohydrodynamics, Comput. Methods Appl. Mech. 190 (2001) 5867–5892.
- [10] L. Seungsoo, G.S. Dulikravich, Magnetohydrodynamic steady flow computation in three dimensions, Int. J. Numer. Methods Fluids 13 (1991) 917–936.
- [11] T.W.H. Sheu, R.K. Lin, Development of a convection-diffusion-reaction magnetohydrodynamic solver on nonstaggered grids., Int. J. Numer. Methods Fluids 45 (2004) 1209–1233.
- [12] M. Dehghan, D. Mirzaei, Meshless local boundary integral equation (LBIE) method for the unsteady magnetohydrodynamic (MHD) flow in rectangular and circular pipes, Comput. Phys. Comm. 180 (2009) 1458–1466.

- [13] M. Dehghan, D. Mirzaei, Meshless local Petrov-Galerkin (MLPG) method for the unsteady magnetohydrodynamic (MHD) flow through pipe with arbitrary wall conductivity, *Appl. Numer. Math.* 59 (2009) 1043–1058.
- [14] V.C. Loukopoulos, G.C. Bourantas, E.D. Skouras, G.C. Nikiforidis, Localized meshless point collocation method for time-dependent magnetohydrodynamics flow through pipes under a variety of wall conductivity conditions, *Comput. Mech.* 47 (2011) 137–159.
- [15] C. Bozkaya, M. Tezer-Sezgin, Boundary element solution of unsteady magnetohydrodynamic duct flow with differential quadrature time integration scheme, *Int. J. Numer. Methods Fluids* 51 (2006) 567–584.
- [16] N. Bozkaya, M. Tezer-Sezgin, Time-domain BEM solution of convection-diffusion type MHD equations, *Int. J. Numer. Methods Fluids* 56 (2008) 1969–1991.
- [17] U.S. Mahabaleshwar, I. Pažanin, M. Radulović, F.J. Suárez-Grau, Effects of small boundary perturbation on the MHD duct flow, *Theor. Appl.* 44 (2017) 83–101.
- [18] E. Marušić-Paloka, I. Pažanin, On the Darcy-Brinkman flow through channel with slightly perturbed boundary, *Transp. Porous Med.* 117 (2017) 27–44.
- [19] W. Jäger, A. Mikelić, On the roughness-induced effective boundary conditions for an incompressible viscous flow, *J. Differential Equations* 170 (2001) 96–122.
- [20] C. Aydın, M. Tezer-Sezgin, DRBEM solution of the Cauchy MHD duct flow with a slipping perturbed boundary, *Eng. Anal. Bound. Elem.* 93 (2018) 94–104.
- [21] P.W. Partridge, C.A. Brebbia, L.C. Wrobel, *The Dual Reciprocity Boundary Element Method*, Computational Mechanics Publications, Southampton Boston, 1992.
- [22] C.L.N. Cunha, J.A.M. Carrer, M.F. Oliveira, V.L. Costa, A study concerning the solution of advection-diffusion problems by the Boundary Element Method, *Eng. Anal. Bound. Elem.* 65 (2016) 79–94.
- [23] K.M. Singh, M. Tanaka, Dual reciprocity boundary element analysis of transient advection-diffusion, *Internat. J. Numer. Methods Heat* 13 (2003) 633–646.